JOURNAL OF ELECTROMAGNETIC ENGINEERING AND SCIENCE, VOL. 17, NO. 1, 1~8, JAN. 2017

http://dx.doi.org/10.5515/JKIEES.2017.17.1.1
ISSN 2234-8395 (Online) · ISSN 2234-8409 (Print)

Broadband Characterization of Circularly Polarized Waveguide Antennas Using L-Shaped Probe

(*Invited Paper*)

Takeshi Fukusako*

Abstract

This paper introduces a technique to obtain the broadband characteristics of circularly polarized antennas using an L-shaped probe. A waveguide antenna is suitable for obtaining high gain and handling convenience in some applications; however, the asymmetrical structure of the L-shaped probe results in cross-polarization and frequency dependence on the field distribution of higher-order modes (HOM). In addition to the basic characteristics of a waveguide antenna with an L-shaped probe, the author discusses some techniques to reduce the HOM and cross-polarization. As a result, the 3-dB axial ratio (AR) is obtained with the fundamental mode even when the frequency is expanded to the region for HOM of TM. This reduction is mainly due to the cutoff structure to the TM mode around the short wall of the waveguide. Furthermore, some aperture modification techniques can reduce the cross-polarization in a wide range of angles in the radiation pattern. Such techniques and their mechanisms are discussed in this paper. The obtained performance shows that the proposed antennas have a wide range of angles of 3-dB AR in the radiation pattern, broadband characteristics in impedance and AR, and low variation in group velocity.

Key Words: Broadband Characteristics, Circular Polarization, L-Shaped Probe, Waveguide Antenna.

I. INTRODUCTION

Circularly polarized (CP) antennas have been widely used in many applications such as global positioning systems, satellite communication, RADAR, radio astronomy, and RFID systems. Circular polarization affords two main advantages in such applications: it avoids polarization misalignment as the electric field (E-field) rotates, and it reduces multipath fading because as long as the incident wave angle is less than the Brewster angle, the reflected CP wave has reversed rotation direction, resulting in cross-polarization (XPOL) [1–3].

CP radiation can be obtained under the condition that two orthogonal modes are generated with equal amplitude and 90° phase difference. For example, two typical methods, the one- and two-point feeding methods, are well known to circularly polarize patch antennas. In addition, the normal and axial modes of helix antennas are well known [4, 5]. The spiral antenna technique is well known as a broadband CP antenna using a travelling wave [6–8]; however, the dispersive characteristics must be considered when a pulse signal is required for RADAR and UWB systems [9]. Signal processing can be used to avoid the effect of the characteristics. However, such processing is not suitable for high-speed communications. Therefore, wideband CP antennas with non-dispersive characteristics are required.

Manuscript received December 21, 2016 ; Accepted January 17, 2017. (ID No. 20161221-049J)
Department of Computer Science and Electrical Engineering, Kumamoto University, Kumamoto, Japan.
*Corresponding Author: Takeshi Fukusako (e-mail: fukusako@cs.kumamoto-u.ac.jp)

For this purpose, broadband CP antennas require broadband impedance and axial ratio (AR) characteristics as well as constant gain and group delay characteristics. In addition, it is important to avoid multipaths. Furthermore, low XPOL resulting in low AR is needed over a wide range of angles in the radiation pattern.

Recently, several techniques for obtaining CP radiation in a wideband have been studied. Some give low Q value to obtain wideband 3-dB AR bandwidth and impedance [10–12]. A study showed that a metasurface structure called an artificial ground structure (AGS) that consists of a periodic structure on a planar substrate can work as an artificial magnetic conductor [13] and a polarizer [14]. The AGS can extend the AR bandwidth of CP patch antennas [15, 16].

High-gain antennas with broadband AR have also attracted research interest. The author has proposed some broadband CP waveguide antennas using an L-shaped probe [17, 18]. By using the fundamental mode, 3-dB AR bandwidth of around 24% can be achieved easily. This AR bandwidth can be extended by suppressing higher-order modes. Some broadband waveguide CP antennas using an L-shaped probe have been presented in [19–21]. Compared to these planar slot structures, waveguide antennas can achieve broadband performance and high gain and easily yield circular polarization covering a wide azimuth range in the radiation pattern. The author has discussed how such antennas can achieve the required performance mentioned above [22–25].

Ⅱ. Reduction of Higher-Order Modes

An L-shaped probe used to feed the waveguide antenna causes circular polarization with wideband characteristics. Fig. 1 shows an example of a waveguide antenna with a horn and an L-shaped feeding probe. In this structure, the horn antenna was designed using conventional formulas for obtaining an antenna gain of 17 dBi. In addition, an L-shaped probe was installed to generating circular polarization.

In Fig. 1, a metallic ring is embedded deep inside the waveguide. Fig. 2 shows the AR characteristics in the antenna boresight. If this metallic ring is removed, the 3-dB AR bandwidth in the boresight will be about 25% [17, 18]. In the frequency between around the cutoff frequency of TE_{11} (6.51 GHz) and the first higher-order mode (HOM) of TM_{01} (8.51 GHz) modes, the AR exceeds 3 dB. The proposed antenna has an asymmetrical structure in the cross section; therefore, the HOM can easily exist in the waveguide, and the field distribution depends on the frequency. Therefore, in the frequency region of the HOM, maintaining low AR is difficult. For wideband CP antennas, it is important to reduce HOM. For example, in the case of CP antennas, having

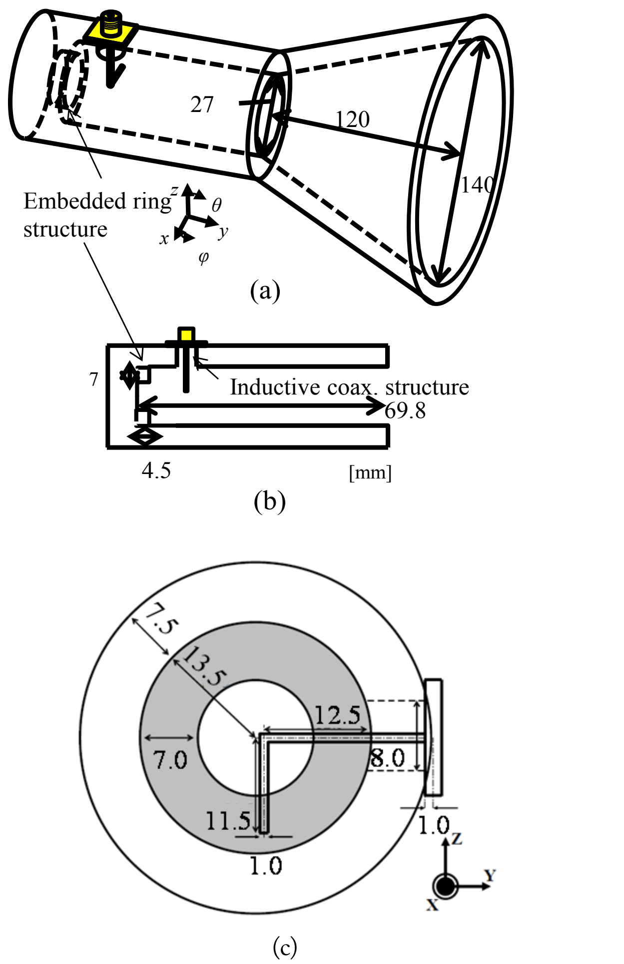

Fig. 1. Antenna structure. (a) Bird's-eye view, (b) side view of the waveguide and (c) front view of the waveguide.

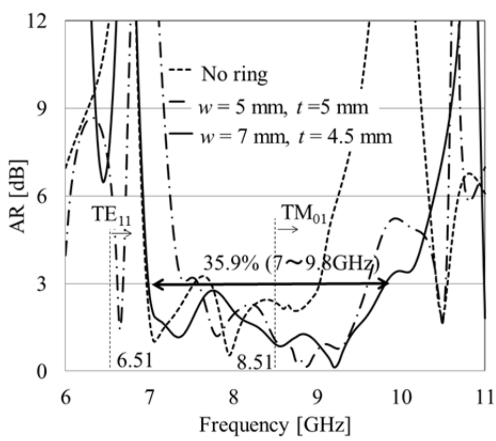

Fig. 2. Axial ratio characteristics in the boresight direction.

a symmetrical structure such as 4-point feeding can reduce the HOM of TM_{21} modes even though TE_{11} is the fundamental mode.

Therefore, for expanding the wideband AR characteristics, the HOM should be removed. For this purpose, we use the embedded metallic ring. By choosing the dimensions of w and t, AR can be reduced effectively in the frequency region

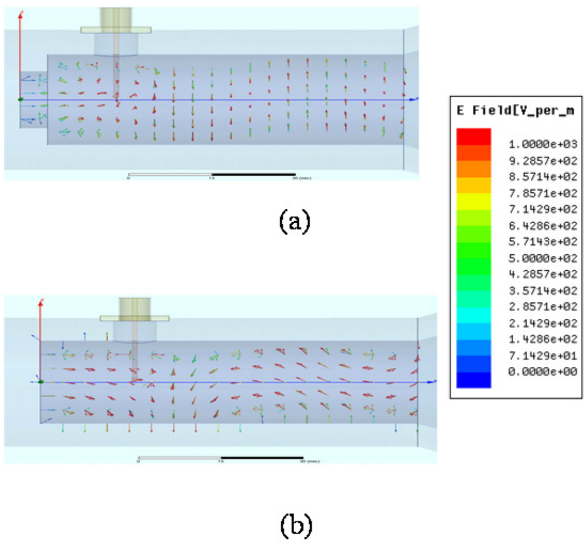

Fig. 3. Electric field distributions in waveguide (a) with and (b) without ring structure.

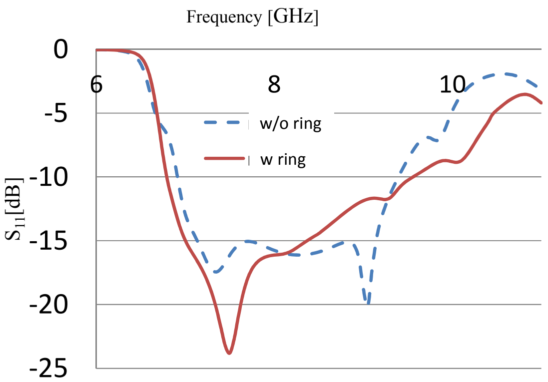

Fig. 4. S_{11} characteristics with and without ring.

of >8.51 GHz. This is probably because HOM of the TM_{01} mode is removed.

To confirm this behavior, we examine the distribution of the E-field at 9 GHz (HOM band) as shown in Fig. 3. In the waveguide with no ring, shown in Fig. 3(a), the E-field in some parts has components parallel to the propagation direction. This indicates that the field includes the TM_{01} mode considering the frequency. On the other hand, when the metallic ring is installed as shown in Fig. 3(b), the E-field in all parts has no component parallel to the propagation direction. We understand that only the TE mode can exist in the waveguide, which contributes to generate CP. CP from the L-shaped probe is generated on the principle that the phase of the current on the probe side along x lags by 90° compared to that along z. This situation can be observed by covering a wideband of 35.9% for 3-dB AR when $w = 7$ mm and $t = 4.5$ mm, as shown in Fig. 2. On the other hand, the ring has only a small effect on the S_{11} characteristics, as shown in Fig. 4. Furthermore, as shown in Fig. 5, the antenna gain is

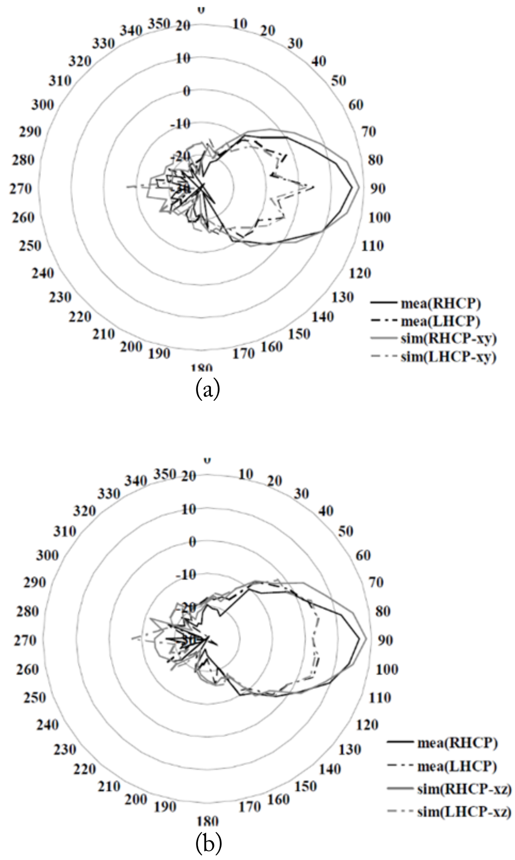

Fig. 5. Radiation patterns in (a) xy-plane and (b) xz-plane at 9 GHz.

around 17 dBic (simulated) and 15 dBic (measured) with sufficiently low XPOL.

III. Enhancement of AR Bandwidth and Angle of CP Radiation

This section discusses some techniques to enhance the AR and angle of CP radiation in radiation patterns. For this purposes, HOM should be reduced. This is an important problem in broadband antennas with an asymmetrical structure, like this structure including the L-shaped probe, because the field of the HOM depends on the frequency. When designing a broadband antenna, it is important to keep a certain field with respect to the frequency. On the other hand, the field of HOM depends on frequency, resulting in limiting the constant characteristics in terms of frequency.

Fig. 6 shows a broadband waveguide antenna structure using the L-shaped probe, where we have installed a step in the aperture. Fig. 7 shows the effect of the aperture step. Fig. 7(a) shows an E-field distribution at 10 GHz in the structure in which the aperture step is removed. In this figure, we see that some E-field vectors have a component parallel to the propagation direction. This indicates that the HOM of the TM mode is included. On the other hand, Fig. 7(b) shows that installing an aperture step in around a location where the

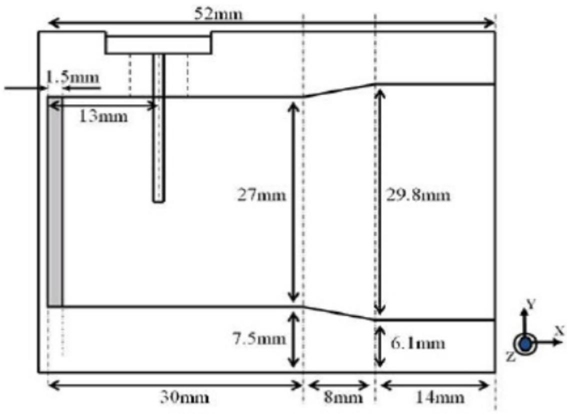

Fig. 6. Structure of antenna [18].

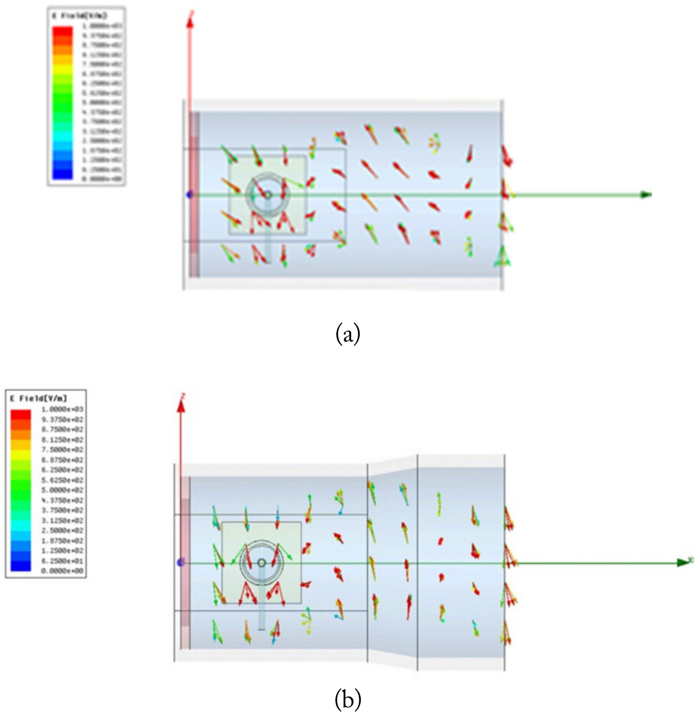

Fig. 7. Effect of aperture step on E-field distribution. (a) Non-stepped aperture antenna and (b) stepped aperture.

TM mode seems strong can control the E-field distribution and make all E-fields directed normal to the wall. This indicates that the HOM of the TM mode has vanished.

Choosing the location of the aperture step is important for this improvement. For building this stepped structure, we choose a location where the TM mode seems strong. If we simply install the step near the aperture, a similar effect will not be produced. In fact, the effect of the aperture step can be seen in the AR characteristics. Fig. 8 shows the AR characteristics for structures with both stepped and non-stepped apertures. AR is seen to be improved at higher frequencies around 10 GHz because the HOM has been reduced around this frequency.

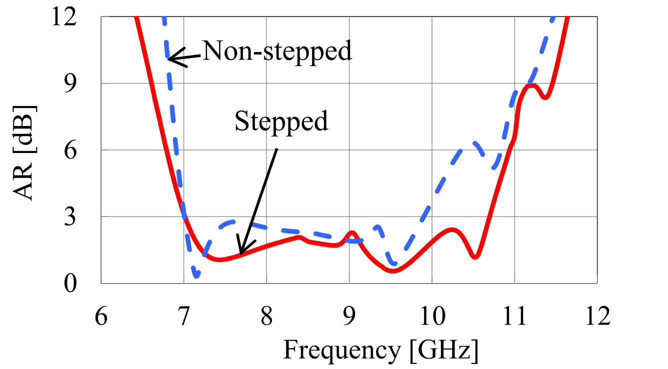

Fig. 8. Axial ratio characteristics in the boresight direction of the antennas with stepped and non-stepped aperture.

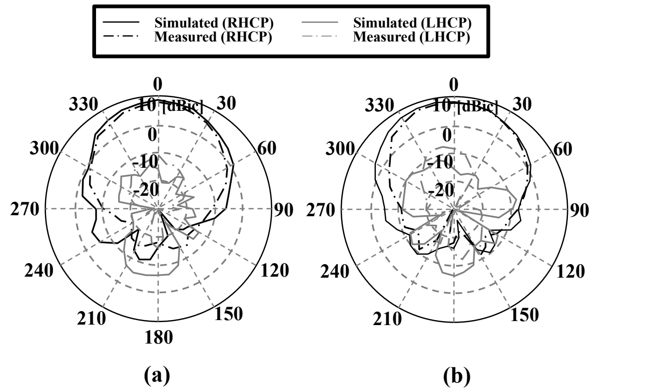

Fig. 9. Radiation pattern of antenna with stepped aperture at 7.5 GHz in (a) xy-plane and (b) zx-plane.

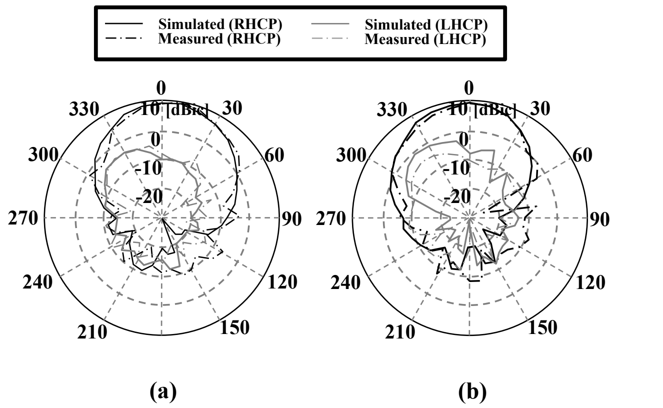

Fig. 10. Radiation pattern of antenna with stepped aperture at 10.25 GHz in (a) xy-plane and (b) zx-plane.

Fig. 9 shows the radiation patterns at 7.25 GHz. At around this frequency, the XPOL has been reduced sufficiently. For up to around 9.5 GHz, the radiation patterns show similar XPOL. However, at around 10.25 GHz, the XPOL is enhanced in a wide range of angles, as shown in Fig. 10.

As mentioned in the introduction, a wide range of CP radiation is required for applications such as RADAR. Such applications also require high gain. Therefore, a waveguide CP antenna is discussed in the next section.

Ⅳ. Suppression of Cross-Polarization over a Wide Range of Angles

Fig. 11 shows another circular waveguide antenna structure with a curved short wall [25]. The curved short wall has a parabolic surface with $x = 0.08(y^2 + z^2)$ mm. In this structure, the position of the short wall along the x-axis affects the impedance matching. Therefore, the center position of the curved short wall, the deepest point from the aperture, should be optimized along the x-axis. This parabolic wall serves to suppress XPOL over a wide range of angles in the radiation pattern because the distance between the wall and the bent point of the L-shaped probe can be almost constant with respect to any angle centered on the bent point. This suppresses XPOL. Furthermore, the parabolic wall can also suppress the HOM of the TM_{01} mode because the parabolic shape can give a cut-off frequency for the HOM near the wall.

Fig. 12 shows the S_{11} characteristics. The −10 dB S_{11} bandwidth of the proposed and previous antennas are 40.7% (6.85–10.35 GHz) and 43.7% (6.8–10.6 GHz), respectively. The S_{11} bandwidth of the proposed antenna is slightly narrow at higher frequency, even though the probes shown in both Figs. 13 and 14 are identical.

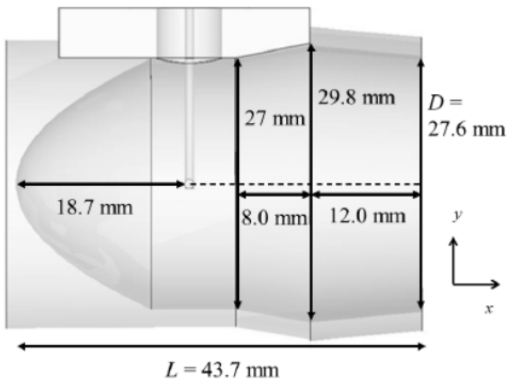

Fig. 11. Waveguide antenna using an L-shaped probe and parabolic short wall [25].

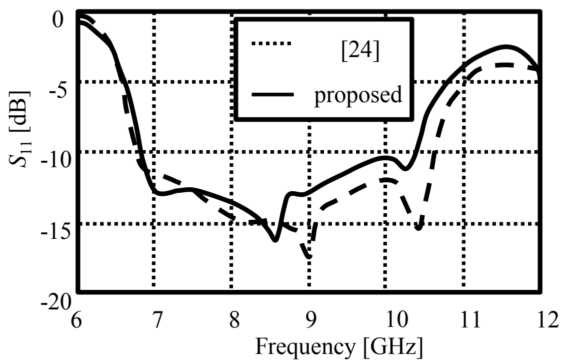

Fig. 12. Comparison of S_{11} characteristics of antennas with both parabolic and ring walls.

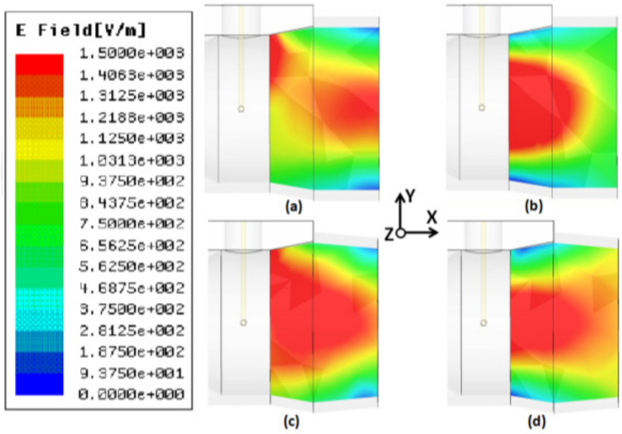

Fig. 13. E-field distribution with magnitude expression in the xy-plane at 7.5 GHz. (a) ωt=0° for D=29.8 mm, (b) ωt=90° for D= 29.8 mm, (c) ωt=0° for D=27.6 mm, and (d) ωt=90° for D =27.6 mm.

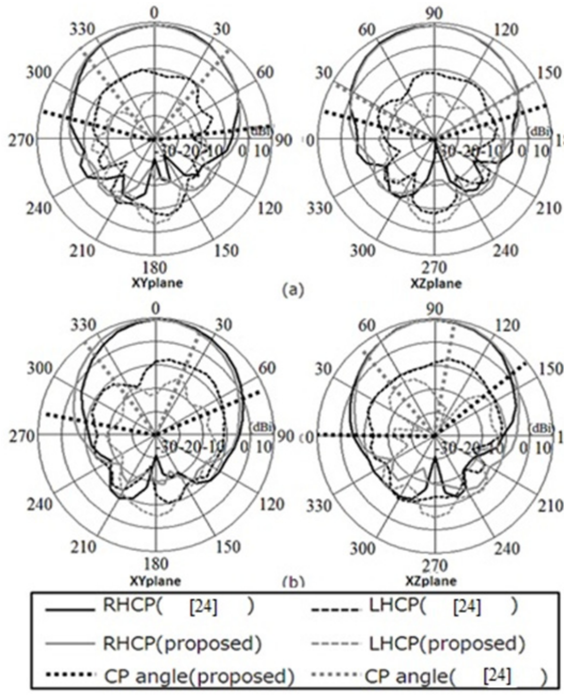

Fig. 14. Comparison of radiation patterns at (a) 8 GHz and (b) 9 GHz.

Fig. 15 shows the 3-dB AR characteristics. The AR bandwidth of the proposed antenna is narrower than that of the previous antenna; however, the AR value is lower than that of the previous antenna. This result indicates that XPOL in the boresight direction decreases.

Next, the reason why the AR at low frequency is reduced when the aperture is smaller is discussed. Fig. 13 shows the

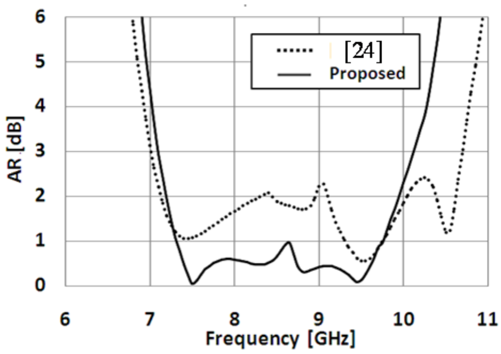

Fig. 15. Comparison of axial ratio (AR) characteristics.

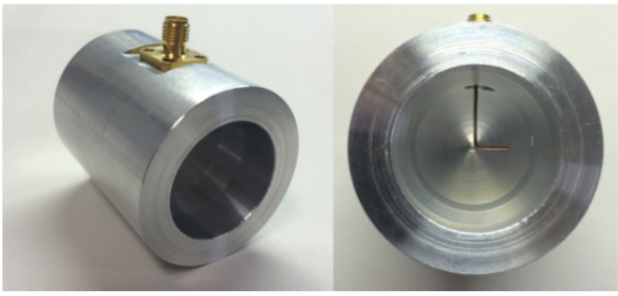

(a) (b)

Fig. 16. Photos of fabricated antenna. (a) 3D view and (b) L-shaped probe inside the antenna.

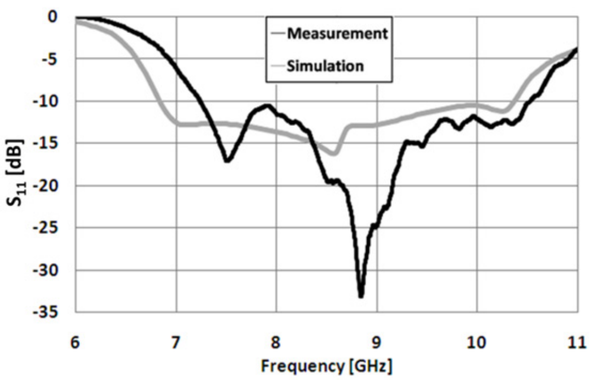

Fig. 17. Measured and simulated S_{11} characteristics.

strength of the E-field distributions in the xy-plane at $\omega t = 0$ (reference) and 90° for $D = 29.8$ mm and 27.6 mm, where ωt is the phase of the input signal. When $D = 29.8$ mm, the E-field intensity is not constant at the center of the aperture; specifically, the E-field is strong at the center when $\omega t = 0°$ but only approximately half as weak when $\omega t = 90°$. We consider that such behavior leads to an increase in AR. On the other hand, for $D = 27.6$ mm, the strength of the E-field is constant at the aperture.

Fig. 14 shows the radiation patterns at 8 and 9 GHz. This figure shows a reduction in XPOL at both the boresight and off-boresight. Therefore, the angle range in which CP is generated is wider than that of the previous antenna.

The simulation and experimental results of the proposed antenna are compared. Fig. 16 shows a photograph of the fabricated antenna. The antenna is made of aluminum, and the L-shaped probe is made of copper.

The measured and simulated S_{11} are similar, as shown in Fig. 17, around 43% at -10 dB; however, the measured 3-dB AR bandwidth is slightly narrower than the simulated one, as shown in Fig. 18.

Fig. 19 shows the simulated and measured radiation patterns at 8 and 9 GHz. The measured and simulated results show good agreement at 8 GHz. The measured and simulated

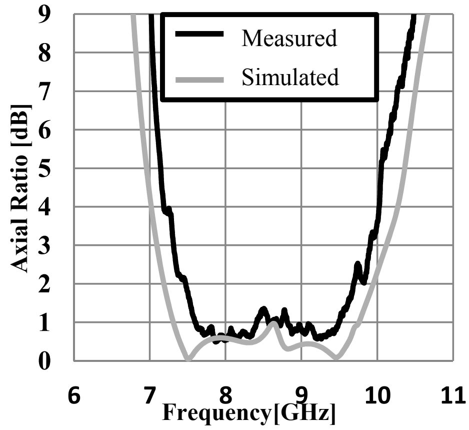

Fig. 18. Simulated and measured results of axial ratio characteristics along the boresight.

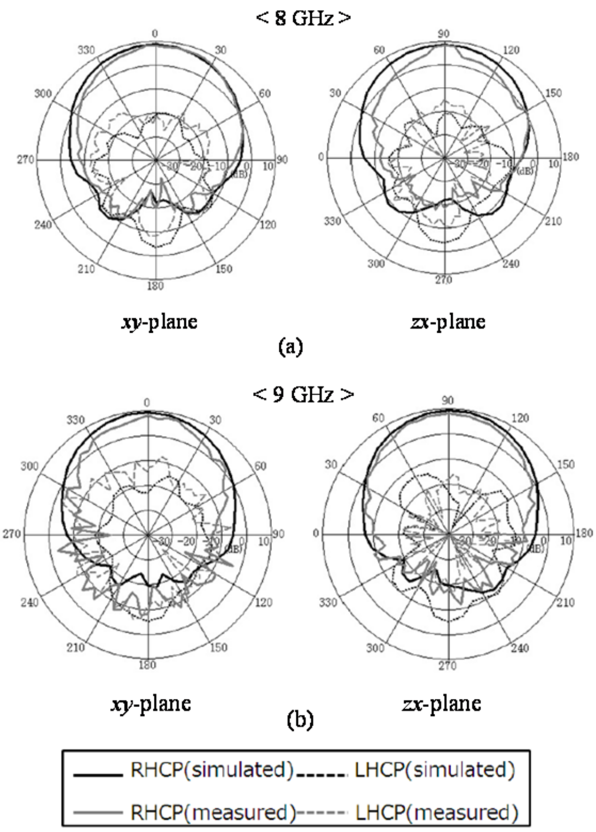

Fig. 19. Radiation patterns.

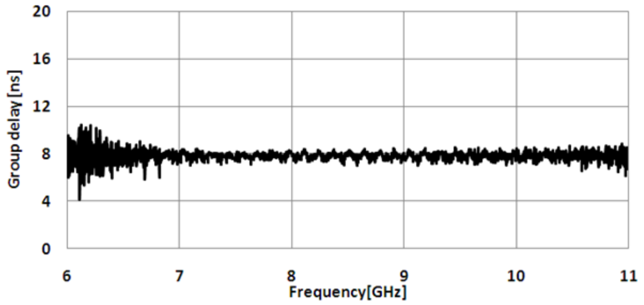

Fig. 20. Group delay characteristics.

XPOL differ slightly; however, XPOL compared to that in [24], as shown in Fig. 8, is kept sufficiently low over a wide range of angles. Furthermore, Fig. 20 shows the mea-sured group delay characteristics in the boresight. The group delay remains almost constant with less than 1-ns variation. This indicates that the proposed antenna could be applied for UWB-high band applications.

V. Conclusions

The author has presented some recent results on broadband CP waveguide antennas using an L-shaped probe. This type of antenna can achieve high gain and constant group velocity in addition to wideband 3-dB AR and impedance characteristics. However, the L-shaped structure has an asymmetrical structure, resulting in high XPOL. The author has shown that XPOL can be reduced by using some techniques. This is partly due to the reduction of HOM, which has an asymmetrical, frequency-dependent distribution. Low XPOL results in a wide range of angles in the radiation pattern. The proposed antenna has 3-dB AR of around 45%, and the azimuth range for 3-dB AR is 100°–170° depending on frequency. Expanding the AR bandwidth while retaining the above advantageous characteristics is important for covering the UWB full band.

References

[1] H. Mott, *Polarization in Antennas and Radar*, New York, NY: Wiley, 1986.

[2] W. L. Stutzman, *Polarization in Electromagnetic Systems*, Boston, MA: Artech House, 1992.

[3] D. Pozar and D. H. Schaubert, *Microstrip Antennas: The Analysis and Design of Microstrip Antennas and Arrays*, Piscataway, NJ: IEEE Press, 1995.

[4] H. A. Wheeler, "A helical antenna for circular polarization," *Proceedings of the IRE*, vol. 35, no. 12, pp. 1484−1488, 1947.

[5] J. D. Kraus, "The helical antenna," *Proceedings of the IRE*, vol. 37, no. 3, pp. 263−272, 1949.

[6] J. D. Dyson, "The equiangular spiral antenna," *IRE Transactions on Antennas and Propagation*, vol. 7, no. 2, pp. 181−187, 1959.

[7] J. A. Kaiser, "The Archimedean two-wire spiral antenna," *IRE Transactions on Antennas and Propagation*, vol. 8, no. 3, pp. 312−323, 1960.

[8] M. S. Wheeler, "On the radiation from several regions in spiral antennas," *IRE Transactions on Antennas and Propagation*, vol. 9, no. 1, pp. 100−102, 1961.

[9] A. E. C. Tan, M. Y. Chia, and K. Rambabu, "Time domain characterization of circularly polarized ultrawideband array," *IEEE Transactions on Antennas and Propagation*, vol. 58, no. 11, pp. 3524−3531, 2010.

[10] F. S. Chang, K. L. Wong, and T. W. Chiou, "Low-cost broadband circularly polarized patch antenna," *IEEE Transactions on Antennas and Propagation*, vol. 51, no. 10, pp. 3006−3009, 2003.

[11] W. K. Lo, J. L. Hu, C. H. Chan, and K. M. Luk, "L-shaped probe-feed circularly polarized microstrip patch antenna with a cross slot," *Microwave and Optical Technology Letters*, vol. 25, no. 4, pp. 251−253, 2000.

[12] K. L. Chung and A. S. Mohan, "A systematic design method to obtain broadband characteristics for singly-fed electromagnetically coupled patch antennas for circular polarization," *IEEE Transactions on Antennas and Propagation*, vol. 51, no. 12, pp. 3239−3248, 2003.

[13] D. Qu, L. Shafai, and A. Foroozesh, "Improving microstrip patch antenna performance using EBG substrates," *IEE Proceedings-Microwaves, Antennas and Propagation*, vol. 153, no. 6, pp. 558-563, 2006.

[14] F. Yang and Y. Rahmat-Samii, "A low profile single dipole antenna radiating circularly polarized waves," *IEEE Transactions on Antennas and Propagation*, vol. 53, no. 9, pp. 3083−3086, 2005.

[15] T. Nakamura and T. Fukusako, "Broadband design of circularly polarized microstrip antenna using artificial ground structure with rectangular unit cells," *IEEE Transactions on Antennas and Propagation*, vol. 59, no. 6, pp. 2103−2110, 2011.

[16] S. Maruyama and T. Fukusako, "An interpretative study on circularly polarized patch antenna using artificial ground structure," *IEEE Transactions on Antennas and Propagation*, vol. 62, no. 11, pp. 5919−5924, 2014.

[17] T. Fukusako, K. Okuhata, K. Yanagawa, and N. Mita, "Generation of circular polarization using rectangular waveguide with L-type probe," *IEICE Transactions on Communications*, vol. 86B, no. 7, pp. 2246−2249, 2003.

[18] T. Fukusako and L. Shafai, "Circularly polarized broadband antenna with L-shaped probe and wide slot," in *Proceedings of 12th International Symposium on Anten-*

na Technology and Applied Electromagnetics (ANTEM) and Canadian Radio Sciences (URSI/CNC), Montreal, Canada, 2006, pp. 445–448.

[19] S. L. S. Yang, A. A. Kishk, and K. F. Lee, "Wideband circularly polarized antenna with L-shaped slot," *IEEE Transactions on Antennas and Propagation*, vol. 56, no. 6, pp. 1780–1783, 2008.

[20] L. Y. Tseng and T. Y. Han, "Microstrip-fed circular slot antenna for circular polarization," *Microwave and Optical Technology Letters*, vol. 50, no. 4, pp. 1056–1058, 2008.

[21] J. S. Row and S. W. Wu, "Circularly polarized wide slot antenna with a parasitic patch," *IEEE Transactions on Antennas and Propagation*, vol. 56, no. 6, pp. 2826–2832, 2008.

[22] S. Yamaura and T. Fukusako, "Bandwidth enhancement of circularly polarized waveguide antenna using L-shaped probe," in *Proceedings of 2011 International Symposium on Antennas and Propagation (ISAP2011)*, Jeju, Korea, 2011.

[23] S. Yamaura and T. Fukusako, "Reduction of cross polarization in higher frequency for circularly polarized broadband antenna with L-shaped probe and parabolic short wall," *IEICE Communications Express*, vol. 2, no. 5, pp. 180–185, 2013.

[24] T. Fukusako, N. Noguchi, and S. Yamaura, "Bandwidth enhancement of circular polarization generated from circular waveguide and L-shaped probe," in *Proceedings of 2013 IEEE International Workshop on Electromagnetics: Application and Student Innovation Competition (iWEM2013)*, Hong Kong, 2013, pp. 5–8.

[25] R. Yamauchi and T. Fukusako, "A broadband circularly polarized waveguide antenna design for low cross-polarization," *IEICE Transactions on Communications*, vol. 99B, no. 10, pp. 2187–2194, 2016.

Takeshi Fukusako

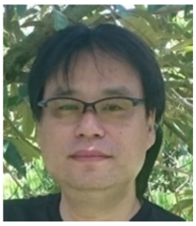

received the B.E., M.E., and Ph.D. degrees in Engineering from Kyoto Institute of Technology, Kyoto, Japan, in 1992, 1994, and 1997, respectively. In 1997, he joined the Kumamoto University, Kumamoto, Japan, as a Research Associate. He is currently working with the Department of Computer Science and Electrical Engineering, Kumamoto University, as a Professor. From 2005 to 2006, he was a Visiting Researcher at the University of Manitoba, Canada. Furthermore, he was a Visiting Associate Professor of the City University of Hong Kong, Hong Kong SAR, China, from March to April 2015. His current research interests include antenna design, especially broadband antennas, circularly polarized antennas, and electrically small antennas, and their applications. He served with *IEICE Transactions on Communications* as an Associate Editor from 2012 to 2016. He has been an Associate Editor of *IEEE Transactions on Antennas Propagation* since 2015. In 2014, he served as one of the TPC co-chairs at the 2014 IEEE International Workshop on Electromagnetics: Applications and Student Innovation Competition (iWEM2014), and in 2017, he will serve as one of the general chairs of IEEE International Conference on Computational Electromagnetics (ICCEM2017). He is a Senior Member of IEEE and a Senior Member of IEICE.